

Anti-Inflammatory Meroterpenoids of *Cordia glazioviana* (Boraginaceae)

Ana Karine O. Silva,^{1b} Francisco C. L. Pinto,^{1b} Kirley M. Canuto,^{1b} Raimundo Braz-Filho,^{1c}
Rose Anny C. Silva,^{1d} Flávia A. Santos,^{1e} Norberto K. V. Monteiro,^{1f} Edilberto R. Silveira^{1a} and
Otilia D. L. Pessoa^{1*,a}

^aDepartamento de Química Orgânica e Inorgânica, Universidade Federal do Ceará,
60021-970 Fortaleza-CE, Brazil

^bEmbrapa Agroindústria Tropical, 60511-110 Fortaleza-CE, Brazil

^cDepartamento de Química, Universidade Estadual do Norte Fluminense Darcy Ribeiro,
28013-602 Campos dos Goytacazes-RJ, Brazil

^dDepartamento de Medicina Clínica, Universidade Federal do Ceará,
60430-140 Fortaleza-CE, Brazil

^eDepartamento de Fisiologia e Farmacologia, Universidade Federal do Ceará,
60165-085 Fortaleza-CE, Brazil

^fDepartamento de Química Analítica e Físico-Química, Universidade Federal do Ceará,
60461-970 Fortaleza-CE, Brazil

The phytochemical reinvestigation from the heartwood of the extracts of *Cordia glazioviana* led to the isolation of four still undescribed hydroquinones derivatives designated as cordiaquinol D (**1**), cordiaquinol E (**2**), (10*R*)-10,11-dihydrofuran-1,4-dihydroxy-globiferin (**3**) and 2-[(1'*E*,6'*E*)-3',8'-dihydroxy-3',7'-dimethylocta-1',6'-dienyl]-benzene-1,4-diol (**4**), along with the naphthoquinone 6-[(2'*R*)-2'-hydroxy-3',6'-dihydro-2*H*-pyran-5'-yl]-2-methoxy-7-methylnaphthalene-1,4-dione (**5**). Additionally, six previously known compounds were also isolated: *rel*-1,4-dihydroxy-8 α ,11 α ;9 α ,11 α -diepoxy-2-methoxy-8 $\alpha\beta$ -methyl-5,6,7,8,8a,9,10,10a-octahydro-10-antracenone (**6**), didehydroconicol (**7**), 1 β ,6 β -dihydroxy-7-*epi*-eudesm-3-ene (**8**), 1 β ,6 β -dihydroxy-7-*epi*-eudesm-4(15)-ene (**9**), 10,11-dihydroxybisabolol (**10**), and hamanasal-A (**11**). The structures of the new compounds were assigned by high-resolution mass spectrometry (HRMS) and nuclear magnetic resonance (NMR) analyses. The relative stereochemistry of **3**, **4**, and **5** was improved by quantum mechanical calculations. Eight, out of the eleven isolated compounds (**2-9**), were tested through cellular viability and lipopolysaccharide (LPS)-induced inflammation assays against RAW 264.7 macrophage-like cells. Compounds **3-5** exhibited a stronger effect on LPS-induced NO production (half-maximal inhibitory concentration (IC₅₀) 50.34, 105.83, and 66.73 μ M, respectively).

Keywords: *Cordia glazioviana*, Boraginaceae, hydroquinones, naphthoquinones, anti-inflammatory activity

Introduction

Plants of the genus *Cordia* (Boraginaceae) have been described as a prolific source of bioactive compounds.¹ In fact, several *Cordia* species (*C. dichotoma*, *C. latifolia*, *C. verbenacea*, *C. myxa*, *C. rothii*, *C. gharaf*, *C. obliqua*, etc.) have been used in different traditional systems of

medicine around the world such as the Ayurveda, Unani, and Siddha² due to their ethnopharmacological properties: anti-inflammatory, antimicrobial, anthelmintic, analgesic, and diuretic.¹

Despite the wealthy Brazilian biodiversity, the great traditional knowledge and acceptance of medicinal plants, in contrast to the increasing world demand for phytotherapeutics, the Brazilian herbal medicine market is still very modest. Nevertheless, it is worthwhile to

*e-mail: otillioiola@gmail.com

highlight that an anti-inflammatory product incorporative *Cordia verbenacea* essential oil, is found among the top 20 pharmaceutical drugs marketed in Brazil in 2016.³ Moreover, recent studies have evidenced the anti-inflammatory potential of extracts and pure compounds from other *Cordia* species.⁴

Previous phytochemical studies^{5,6} on *Cordia* genus have reported the isolation of terpenoids, particularly sesquiterpenes and triterpenes, meroterpenoid benzoquinones, and naphthoquinones as well as their respective hydroquinones. Furthermore, the anti-inflammatory effect of sesquiterpenes,⁷ triterpenes,⁸ hydroquinones,⁹ and naphthoquinones¹⁰ have been demonstrated.

Cordia glazioviana (*Auxemma glazioviana*), an endemic Brazilian plant, is largely widespread in the “caatinga” (the characteristic biome of northeastern Brazil).¹¹ In folk medicine, the water decoction from its barks is indicated to the healing of small cuts and wounds.⁶ Previous reports^{6,12} on *C. glazioviana* described the isolation of sesquiterpenes and terpenoids benzoquinones, as well as hydroquinones. Thus, encouraged by the new perspective, we decided to reinvestigate the extracts of *C. glazioviana* pursuing the isolation of anti-inflammatory natural chemical compounds.

Results and Discussion

Eleven meroterpenoid compounds including sesquiterpenes, hydroquinones, and naphthoquinones, five of which previously unreported (**1-5**), were isolated from the ethanol (EtOH) extract of the heartwood of *C. glazioviana* (Figure 1).

Compound **1** had its molecular formula established as C₁₇H₁₈O₅ by high-resolution electrospray ionization mass spectrometry (HRESIMS) through the deprotonated molecule [M – H][–] at *m/z* 301.1076 (calcd. *m/z* 301.1081). Its infrared (IR) spectrum indicated absorption bands for hydroxy (3405 cm^{–1}), carbonyls (1698 and 1630 cm^{–1}), and carbon-carbon double bonds (1490 and 1442 cm^{–1}). The ¹H NMR (nuclear magnetic resonance) spectrum (Table 1) displayed signals for aldehyde δ_H 9.50 (s, H-11), aromatic δ_H 6.41 (s, H-3), methyldiene δ_H 6.38 (s, H-6a), 6.23 (s, H-6b), and vinyl δ_H 4.98 (d, *J* 17.2 Hz) and 4.97 (d, *J* 11.0 Hz) to 2H-7 and 5.80 (dd, *J* 17.2, 11.0 Hz, H-8) protons. Additionally, also displayed proton signals for diastereotopic methylene δ_H 3.05 (d, *J* 17.1 Hz, H-9a) and 2.85 (d, *J* 17.1 Hz, H-9b), a methine proton δ_H 3.94 (1H, s, H-10a), as well as methoxyl δ_H 3.93 (s, OMe-2) and the methyl groups δ_H 1.12 (s, Me-12). The ¹³C NMR spectrum displayed signals for 17 carbon atoms, assigned by heteronuclear single quantum correlation (HSQC) spectra

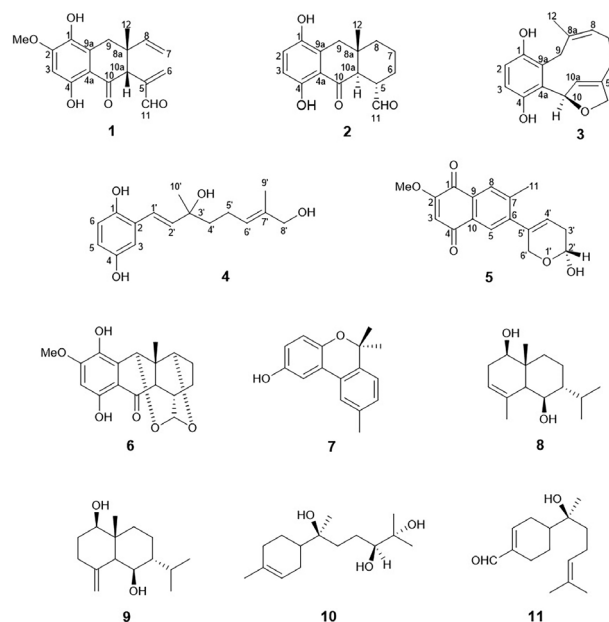


Figure 1. Structures of compounds **1-11**.

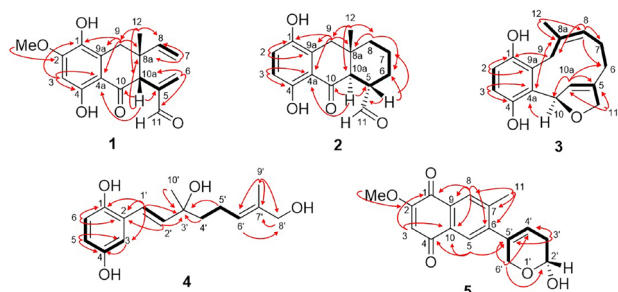
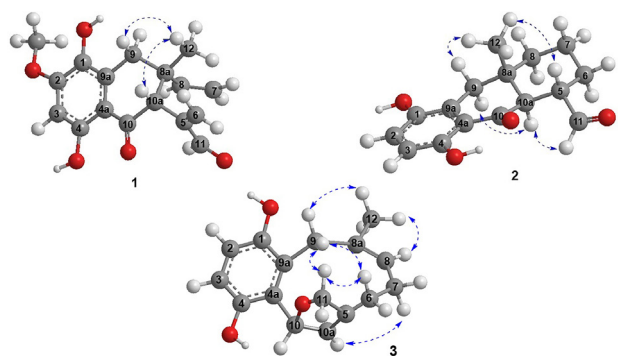
into two methyls (including the methoxyl), two carbons sp³ hybridized (methylene and methine), two double bonds (terminal and vinyl), an aldehyde carbonyl at δ_C 195.5 (C-11) and, comparatively, eight non-hydrogenated carbons, including a conjugated ketone carbonyl at δ_C 202.7 (C-10), Table 1. ¹H and ¹³C NMR data analysis were consistent with a 2-methoxy-*p*-hydroquinone, a vinyl group and an α,β-conjugated propenal moiety. The heteronuclear multiple bond correlation (HMBC) spectrum showed correlations of the methyldiene hydrogens at δ_H 6.38/6.23 (2H-6) with the aldehyde carbonyl at δ_C 195.5 (C-11) and δ_C 55.4 (C-10a), and the proton at δ_H 3.94 (H-10a) with the carbon at δ_C 202.7 (C-10) supporting the propenal moiety at the alpha position of the ketone carbonyl. The stereocenter C-8a, bearing a methyl and a vinyl group, was supported by the HMBC correlations of the methyldiene vinyl protons at δ_H 4.98/4.97 (2H-7) with the carbon at δ_C 42.8 (C-8a), and the methyl protons at δ_H 1.12 (Me-12) with the sp² methine carbon at δ_C 143.3 (C-8). Additional HMBC correlations, as depicted in Figure 2, supported the suggested planar structure. The relative stereochemistry ascribed to the stereocenters C-8a (*R**) and C-10a (*R**) were determined based on the nuclear Overhauser spectrum (NOESY) correlations between H-10a and the Me-12 (Figure 3) indicating that both vinyl and propenal moieties are *cis*-vicinally positioned, what is in agreement with previous compounds isolated from other *Cordia* species.^{5,6} From the above data, the relative configuration of **1**, named cordiaquinol D, was established as shown in Figure 3.

Compound **2** had the molecular formula assigned as C₁₆H₁₈O₄ based on the deprotonated molecule [M – H][–] at

Table 1. ^1H (500 MHz, MeOD) and ^{13}C NMR (125 MHz, MeO) data of compounds **1-3**

Position	1		2		3	
	δ_{C}	δ_{H} multiplicity (J / Hz)	δ_{C}	δ_{H} multiplicity (J / Hz)	δ_{C}	δ_{H} multiplicity (J / Hz)
1	137.6		148.6		151.2	
2	157.3		125.7	7.07 d (8.9)	117.2	6.62 d (8.7)
3	98.4	6.41 s	116.0	6.69 d (8.9)	115.1	6.54 d (8.7)
4	160.2		156.6		149.9	
4a	127.0		117.6		127.3	
5	146.8		46.5	2.68 m	135.4	
6	139.0	6.38 s 6.23 s	28.0	1.97 dd (13.4, 3.5) 1.38 m	28.0	2.11 m 2.06 m
7	114.7	4.98 d (17.2) 4.97 d (11.0)	21.3	1.79 m 1.69 m	25.1	2.30 d (12.2) 1.90 td (12.2, 2.8)
8	143.3	5.80 dd (17.2, 11.0)	41.1	1.79 m 1.69 m	121.4	5.04 t (8.5)
8a	42.8		37.2		143.5	
9	34.4	3.05 d (17.1) 2.85 d (17.1)	41.0	3.07 d (17.1) 2.70 d (17.1)	28.1	3.40 d (14.0) 2.91 d (14.0)
9a	110.7		128.7		128.6	
10	202.7		206.1		83.2	6.67 dd (5.7, 3.6)
10a	55.4	3.94 s	57.1	3.11 d (11.0)	126.9	5.20 br s
11	195.5	9.50 s	205.7	9.81 d (3.4)	77.5	4.75 dd (12.0, 5.7) 4.69 ddd (12.0, 3.6, 2.8)
12	26.5	1.12 s	18.2	0.88 s	22.4	1.59 s
2-OMe	56.8	3.93 s				

s: singlet; d: doublet; t: triplet; m: multiplet; br s: broad singlet; dd: doublet of doublets; td: triplet of doublets; ddd: doublet of doublet of doublets.

**Figure 2.** COSY (—) and HMBC (H → C) correlations of **1-5**.**Figure 3.** Stick and ball structures of **1-3** depicting the key NOESY correlations of **1-3**.

m/z 273.1129 (calcd. m/z 273.1132) in the HRESIMS spectrum. Its IR spectrum displayed absorption bands for hydroxy (3412 cm^{-1}), carbonyls (1674 and 1631 cm^{-1}), and aromatic ring (1467 cm^{-1}). The ^1H NMR spectrum exhibited signals for aldehyde δ_{H} 9.81 (d, J 3.4 Hz, H-11), *ortho*-positioned protons at δ_{H} 7.07 (d, J 8.9 Hz, H-2) and 6.69 (d, J 8.9 Hz, H-3), two methines δ_{H} 2.68 (m, H-5) and 3.11 (d, J 11.0 Hz, H-10a), one methyl δ_{H} 0.88 (s, Me-12), signals for diastereotopic methylene δ_{H} 3.07 (d, J 17.1 Hz, H-9a) and 2.70 (d, J 17.1 Hz, H-9b), and a series of methylene protons at δ_{H} 1.28-1.97. The ^{13}C NMR spectrum showed 16 carbon signals assigned by distortionless enhancement by polarization transfer (DEPT 135°) and HSQC spectra into one methyl, four methylenes, two methines, two hydrogenated benzene, and seven non-hydrogenated carbon atoms, two of which related to carbonyls at δ_{C} 205.7 (C-11) and 206.1 (C-10) for an aldehyde and a ketone, respectively. The ^1H and ^{13}C NMR data were consistent with a 1,4-hydroquinone similar to **1**, but bearing a third ring which could be formed from **1** by the cyclization at C-6/C-7. Similarly, to **1** the aldehyde and the ketone functions, as well as the methyl

group were positioned at C-5, C-10, and C-8a, respectively, in agreement with the HBMBC correlations as summarized in Figure 2. The NOESY spectrum acquired in pyridine (C_5D_5N), Figure S16, Supplementary Information (SI) section showed correlations of the β -oriented methyl group (Me-12) with the methine proton H-5 and with one proton of the diastereotopic methylene H-9 β (δ_H 3.07 d, J 17.1 Hz), indicated an α -orientation for the aldehyde group, while the dipolar interaction of the aldehyde proton (H-11) with the methine proton H-5 and this with the diastereotopic methylene H-9 α (δ_H 2.70 d, J 17.1 Hz) confirmed the α -orientation for the aldehyde function and *trans*-configuration of H-10a relatively to the Me-12 (Figure 3). Thus, the structure of compound **2** was established and designated of cordiaquinol E.

The molecular formula of $C_{16}H_{18}O_3$ of compound **3** was deduced through the protonated molecule $[M + H]^+$ at m/z 259.1418 (calcd. m/z 259.1429), as observed by HRESIMS. The 1H and ^{13}C NMR data were similar to those of the globiferin,¹³ but with the quinoid nucleus in the reduced form. This moiety was evidenced by the *ortho*-positioned hydrogens at δ_H 6.62 (d, J 8.7 Hz, H-2) and 6.54 (d, J 8.7 Hz, H-3) and the chemical shifts at δ_C 151.2 (C-1), 117.2 (C-2), 115.1 (C-3), 149.9 (C-4),

127.3 (C-4a) and 128.6 (C-9a) related to the benzenoid ring. Based on the 1H and ^{13}C NMR data (Table 1) in comparison with those of globiferin,¹³ the structure of **3** was assigned 10,11-dihydrofuran-1,4-dihydroxy-globiferin. Interpretation of the NOESY spectrum, assisted by the three-dimensional molecular structure of **3** built by molecular model, showed correlations for the δ_H 1.59 (Me-12) with δ_H 3.40 (d, J 14.0 Hz, H-9) and δ_H 5.04 (t, J 8.5 Hz, H-8), between δ_H 5.20 (br s, H-10a) and δ_H 1.90 (td, J 12.2, 2.8 Hz, H-7), and among the protons δ_H 2.11 (m, H-6), δ_H 2.91 (d, J 14.0 Hz, H-9) and δ_H 4.75 (dd, J 12.0, 5.7 Hz, H-11) suggesting an *R*-configuration for the stereocenter-C10 which was supported by theoretical calculation methods. For the isomers **3a** (10*S*) and **3b** (10*R*), the calculated ^{13}C chemical shift ($\delta_{C_{calc}}$) values were determined using gauge independent atomic orbital (GIAO)¹⁴ method with mPW1PW91/6-31G(d,p) level of theory whose predicted values are reported in Table 2 in comparison to the experimental ^{13}C chemical shifts ($\delta_{C_{exp}}$). The results obtained (Figure 4) indicated that the coefficients of determination (R^2) between the calculated and experimental data from linear regression analysis were 0.9927 (Figure 4a) and 0.9947 (Figure 4b) for **3a** and **3b**, respectively, suggesting **3b** (10*R*) as the presumable

Table 2. Calculated ^{13}C nuclear magnetic shielding ($\delta_{C_{calc}}$) using GIAO method with mPW1PW91/6-31G(d,p) level of theory for isomers **3a** (10*S*)/**3b** (10*R*), and **5a** (2'*S*)/**5b** (2'*R*) and ^{13}C NMR experimental data ($\delta_{C_{exp}}$)

C	$\delta_{C_{exp}}$	$\delta_{C_{calc}}$		$\Delta\delta_C^a$		C	$\delta_{C_{exp}}$	$\delta_{C_{calc}}$		$\Delta\delta_C^a$	
		3a (<i>S</i>)	3b (<i>R</i>)	3a	3b			5a (<i>S</i>)	5b (<i>R</i>)	5a	5b
1	151.2	145.4611	144.6314	5.7389	6.5686	1	181.3	181.7422	181.6627	-0.4422	-0.3627
2	117.2	108.9535	110.7789	8.2465	6.4211	2	162.3	155.7953	155.8319	6.5047	6.4681
3	115.1	109.2763	109.7169	5.8237	5.3831	3	110.8	113.4709	113.3995	-2.6709	-2.5995
4	149.9	140.7750	144.7028	9.1250	5.1972	4	186.5	181.9432	182.0051	4.5568	4.4949
4a	127.3	127.8443	125.4793	-0.5443	1.8207	5	127.5	122.6102	121.9106	4.8898	5.5894
5	135.4	138.3312	141.4512	-2.9312	-6.0512	6	147.1	143.5774	143.8816	3.5226	3.2184
6	28.0	30.0751	26.9964	-2.0751	1.0036	7	143.9	140.2711	139.6327	3.6289	4.2673
7	25.1	35.5280	30.1266	-10.428	-5.0266	8	129.3	128.1594	128.2636	1.1406	1.0364
8	121.4	122.2173	118.9525	-0.8173	2.4475	9	131.4	126.4381	126.0063	4.9619	5.3937
8a	143.5	141.0534	138.1829	2.4466	5.3171	10	131.4	125.7014	125.7225	5.6986	5.6775
9	28.1	33.3114	31.9102	-5.2114	-3.8102	11	20.4	22.8705	22.9907	-2.4705	-2.5907
9a	128.6	122.0950	124.1246	6.5050	4.4754	2'	92.4	88.4461	93.0382	3.9539	-0.6382
10	83.2	85.6513	83.3143	-2.4513	-0.1143	3'	32.6	32.3276	32.4575	0.2724	0.1425
10a	126.9	127.0580	120.2239	-0.1580	6.6761	4'	123.9	123.9666	127.899	-0.0666	-3.999
11	77.5	78.4126	78.4776	-0.9126	-0.9776	5'	137.8	136.0568	135.1095	1.7432	2.6905
12	22.4	31.9853	23.5382	-9.5853	-1.1382	6'	64.9	60.6239	67.1126	4.2761	-2.2126
						2-OMe	57.3	60.0429	60.0452	-2.7429	-2.7452
sDP4+ / %		0	100			sDP4+ / %		58.71	41.29		
uDP4+ / %		4.53	95.47			uDP4+ / %		0.44	99.56		
DP4+ / %		0	100			DP4+ / %		0.62	99.38		

^a $\Delta\delta = \delta_{C_{exp}} - \delta_{C_{calc}}$: calculated ^{13}C nuclear magnetic shielding deviation. sDP4+: scaled DP4+; uDP4+: unscaled DP4+; DP4+: direct probability 4.

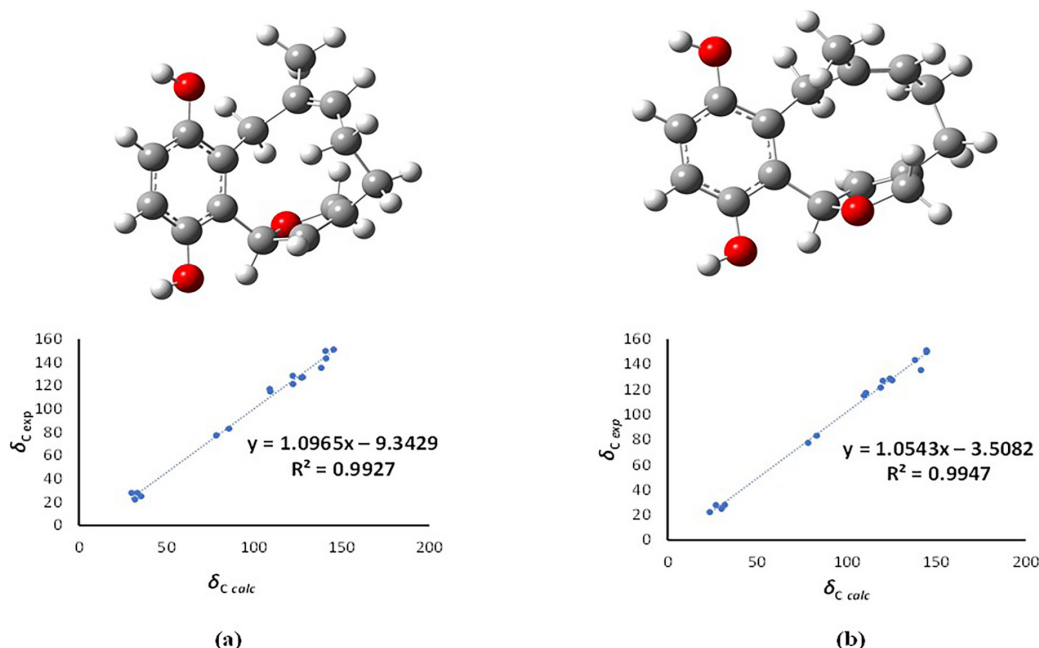


Figure 4. Optimized geometries and coefficient of determination between the experimental chemical shifts ($\delta_{C^{exp}}$) versus calculated chemical shifts ($\delta_{C^{calc}}$) of isomers of compound **3** (10S (**3a**) and 10R (**3b**)) corresponding to figures (a) and (b), respectively.

compound. To confirm this statement, a complementary analysis using DP4+ modified probability analysis was performed.¹⁵ Based on the unscaled DP4+ (uDP4+), scaled DP4+ (sDP4+), and DP4+ probabilities, the isomer **3b** (Table 2) was confirmed. Thus, the structure of **3** was established as (10*R*)-10,11-dihydrofuran-1,4-dihydroxy-globiferin.

The molecular formula for compound **4** (C₁₆H₂₂O₄) was deduced by a combination of the ¹H and ¹³C NMR spectra (Table 3) and the HRESIMS data, which exhibited a protonated ion peak at *m/z* 243.1381 (calcd. *m/z* 243.1380) corresponding to the loss of two H₂O molecules [M + H – 2H₂O]⁺ in comparison with the original molecular formula. The ¹H NMR spectrum revealed signals of an ABC system for a monosubstituted 1,4-hydroquinone moiety at δ_H 6.54 (d, *J* 8.4 Hz, H-6), 6.53 (dd, *J* 8.4, 2.1 Hz, H-5) and 6.44 (d, *J* 2.1 Hz, H-3), a *trans*-disubstituted double bond δ_H 6.29 (d, *J* 16.4 Hz, H-1') and 5.60 (d, *J* 16.4 Hz, H-2'), an *E*-trisubstituted double bond δ_H 5.25 (t, *J* 7.1 Hz, H-6'), as well as signals for methylene protons δ_H 4.02 (s, 2H-8'), 2.17 (m, 2H-5'), and 1.64 (m, 2H-4') and two methyls at δ_H 1.73 (d, *J* 1.2 Hz, 3H-9') and 1.31 (s, 3H-10'). The ¹³C NMR displayed 16 carbon atoms, whose hydrogenation patterns were defined, through DEPT 135° and HSQC spectra, into six monohydrogenated sp² carbon, three methylenes, two methyls, five non-hydrogenated sp² carbon atoms, including an oxygenated tertiary carbon (Table 3). According to ¹H and the ¹³C NMR data, the difference between **4** and its analogous compound 2-(2*Z*)-(3-hydroxy-3,7-dimethylocta-

Table 3. ¹H (500 MHz, MeOD) and ¹³C NMR (125 MHz, MeOD) data of compounds **4** and **5**

Position	4		5	
	δ_C	δ_H multiplicity (<i>J</i> / Hz)	δ_C	δ_H multiplicity (<i>J</i> / Hz)
1	147.5		181.3	
2	123.2		162.3	
3	113.9	6.44 d (2.1)	110.8	6.20 s
4	152.2		186.5	
5	117.6	6.53 dd (8.4, 2.1)	127.5	7.71 s
6	116.5	6.54 d (8.4)	147.1	
7			143.9	
8			129.3	7.86 s
9			131.4	
10			131.4	
11			20.4	2.44 s
1'	124.1	6.29 d (16.4)		
2'	131.7	5.60 d (16.4)	92.4	5.22 t (4.3)
3'	79.1		32.6	2.51 m
				2.62 m
4'	42.3	1.64 m	123.9	5.69 m
5'	23.5	2.17 m	137.8	
6'	128.7	5.25 t (7.1)	64.9	4.43 ddd (16.0, 4.6, 2.1) 4.28 ddd (16.0, 4.6, 2.4)
7'	135.9			
8'	61.4	4.02 s		
9'	21.6	1.73 d (1.2)		
10'	26.5	1.31 s		
2-OMe			57.3	3.89 s

s: singlet; d: doublet; t: triplet; m: multiplet; dd: doublet of doublets; ddd: doublet of doublet of doublets.

1,6-dienyl)-1,4-benzenediol¹⁶ was the oxymethylene moiety instead of the methyl group at C-7'. Thus, the structure of **4** was characterized as the new geranylated hydroquinone designated as 2-[(1'*E*,6'*E*)-3',8'-dihydroxy-3',7'-dimethylocta-1',6'-dienyl]-benzene-1,4-diol.

The molecular formula C₁₇H₁₅O₅ assigned to compound **5** was determined through the deprotonated molecule [M – H][–] at *m/z* 299.0920 (calcd. 299.0925). The ¹H NMR spectrum displayed signals at δ_H 7.86 (s, H-8), 7.71 (s, H-5), 6.20 (s, H-3), 3.89 (s, OMe-2) and 2.44 (s, Me-11) of a 2-methoxy-1,4-naphthoquinone moiety bearing a methyl group. Additional signals at δ_H 5.69 (m, H-4'), 5.22 (t, *J* 4.3 Hz, H-2'), 4.43 (ddd, *J* 16.0, 4.6, 2.1 Hz, H-6')/4.28 (ddd, *J* 16.0, 4.6, 2.4 Hz, H-6') and 2.51 (m, H-3')/2.62 (m, H-3') correlating with the carbons at δ_C 123.9, 92.4, 64.9 and 32.6, respectively, were suggestive of a 3',6'-dihydro-2*H*-pyran-2'-ol moiety. The ¹³C NMR attached proton test (APT) spectrum exhibited 17 carbon signals further classified by HSQC spectra into two methyls, two methylenes, including an oxymethylene, five monohydrogenated carbons (being a hemiketal and four sp² carbon), and eight non-hydrogenated carbon atoms (Table 3). The 2-methoxy-naphthoquinone framework bearing a 3',6'-dihydro-2*H*-pyran-2'-ol moiety at C-6 was confirmed by the long-range correlations of H-5 with the non-hydrogenated olefinic carbon at δ_C 137.8 (C-5'). The relative configuration of the ketal C-2' as **R** (**5b**) was suggested based on theoretically calculated ¹³C chemical shift (δ_{C,calc}) values in comparison to the experimental ¹³C chemical shifts (δ_{C,exp}), Table 3. The coefficients of determination (R²) of 0.9962 (Figure 5a) and 0.9967 (Figure 5b) were found for

the stereoisomers **5a** and **5b**, respectively, including uDP4+, sDP4+ and DP4+ probabilities values¹⁵ (Table 2), suggest **5b** (2'*R*) as the most plausible compound. Indeed, the H-2' splitting as a triplet δ_H 5.22 (*J* 4.3 Hz) due to the similar *J* values for the axial/equatorial and equatorial/equatorial coupling is in accordance with the suggested stereochemistry through the theoretical calculation. In addition, the ¹³C NMR chemical shift of C-2' at δ_C 92.4 is in agreement with the axial-position (δ_C 90.7) of the hydroxyl *versus* the equatorial-position (δ_C 96.0) as previously observed for compound **13** (*rel*-2''-methoxy-7''-methyl-1'',4''-naphthalendione-(6''→5)-tetrahydropyran-(2eq→O→2ax)-tetrahydropyran-(5'→6''')-2'''-methoxy-7''') in Pessoa *et al.*¹⁷ A similar effect of the ¹³C NMR shielding of axial hydroxy *versus* equatorial hydroxy is also observed for the anomeric carbons of α (δ_C 92.9) and β (δ_C 96.7) glucopyranose.¹⁸ Hence, the structure of **5** was established as 6-[(2'*R*)-2'-hydroxy-3',6'-dihydro-2*H*-pyran-5'-yl]-2-methoxy-7-methyl-naphthalene-1,4-dione (**5**).

Furthermore, the following known compounds were also isolated: *rel*-1,4-dihydroxy-8α,11α;9α,11α-diepoxo-2-methoxy-8αβ-methyl-5,6,7,8,8a,9,10,10a-octahydro-10-antracene (**6**),¹⁷ didehydroconicol (**7**),¹⁹ 1β,6β-dihydroxy-7-*epi*-eudesm-3-ene (**8**),²⁰ 1β,6β-dihydroxy-7-*epi*-eudesm-4(15)-ene (**9**),²¹ 10,11-dihydroxybisabolol (**10**),²² and hamansal-A (**11**)²³ (see Figure 1).

Although there is no experimental support for the biosynthesis of the meroterpenoid 1,4-quinones isolated specifically from *Cordia* species, a reasonable biosynthetic

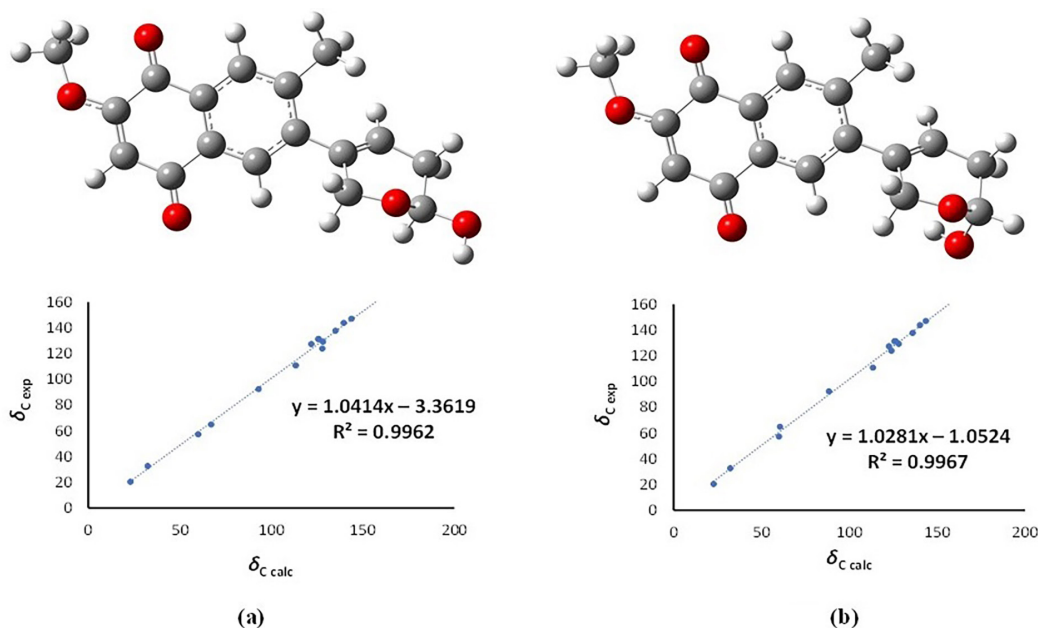


Figure 5. Optimized geometries and coefficient of determination between the experimental chemical shifts (δ_{C,exp}) *versus* calculated chemical shifts (δ_{C,calc}) of isomers of compound **5** (2'*S* (**5a**) and 2'*R* (**5b**)) corresponding to figures (a) and (b), respectively.

pathway for compounds **1** to **6** was suggested based on previous studies reported to terpenoid quinones.²⁴ Thus, it seems reasonable that compounds **1-6** could be produced from a *C*-alkylation of the *p*-hydroxybenzoic acid with two prenyl unities followed by a sequence of typical reactions of the biogenetic process as intramolecular cyclization, oxidation, hydroxylation, and *O*-methylation as depicted in Figure 6.

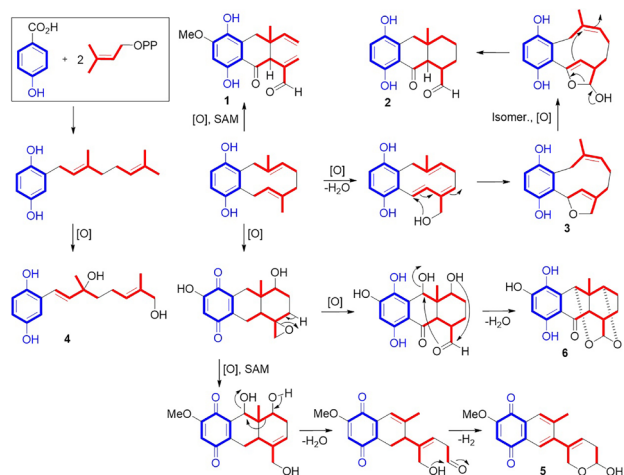


Figure 6. Plausible biogenetic pathways for compounds **1-6**.

3-(4,5-Dimethyl-2-thiazolyl)-2,5-diphenyl-2*H*-tetrazolium bromide (MTT) assay was carried out to evaluate the cytotoxic effects of the compounds on murine macrophages RAW 264.7 cells.²⁵ As shown in Table 4, the compounds demonstrated a reduction of the cellular viability with half-maximal inhibitory concentration (IC_{50}) values between 71.66-1530.02 μ M. The concentrations of 6.125, 12.5, 25, and 50 μ M of compounds (no cytotoxicity on RAW264.7 cells) were selected for the subsequent experiments in the present study.

To evaluate the effects of the isolated compounds on the production of sulfated polysaccharides (LPS)-induced nitric oxide (NO) in RAW264.7 cells, the concentrations of NO in the culture medium were measured by the Griess assay.²⁶ NO levels in the culture supernatants from LPS-stimulated cells were significantly reduced after treatment with the compounds (Table 4). Compounds **3**, **4**, and **5** were more able to reduce NO production with IC_{50} values of 50.34 ± 9.88 , 105.83 ± 5.09 , and 66.73 ± 10.28 μ M, respectively.

Conclusions

Eleven compounds, including four new terpenoid hydroquinones (**1-4**) and a naphthoquinone (**5**), were isolated through the reinvestigation of the EtOH extract

Table 4. Effects of compounds **2-9** on cell viability and inhibiting nitric oxide production in activated RAW264.7 macrophage cells

Compound	Cytotoxicity IC_{50}^a / μ M	NO inhibition IC_{50}^a / μ M
2	158.38 ± 11.05	1420.72 ± 4.63
3	71.66 ± 15.44	50.34 ± 9.88
4	424.82 ± 6.46	105.83 ± 5.09
5	166.25 ± 6.79	66.73 ± 10.28
6	609.48 ± 5.05	143.64 ± 4.67
7	1530.02 ± 4.54	197.68 ± 3.84
8	157.20 ± 6.63	292.04 ± 3.64
9	355.70 ± 10.67	235.50 ± 3.18
Dexamethasone ^b		1.79 ± 0.04

^aHalf-maximal inhibitory concentration (IC_{50}) values are represented as means \pm standard deviation of three independent experiments; ^bpositive control.

from the heartwood of *C. glazioviana*. It is worth highlighting that similar meroterpenoid compounds have been previously isolated from several *Cordia* species, and they seem to be restricted to woody plants, in particular, in the roots and trunk heartwood. As a significant number of terpenoid quinones and hydroquinones were previously isolated from *Cordia* species, it seems reasonable to suggest these compounds as possible chemomarkers for the genus. Eight, out of the eleven isolated compounds (**2-9**), were tested through cellular viability and lipopolysaccharide (LPS)-induced inflammation assays against RAW 264.7 macrophage-like cells, being compound **3** the one that showed the best reduction of the NO synthesis (IC_{50} 50.34 ± 9.88 μ M).

Experimental

General experimental procedures

Optical rotations were measured on a Jasco P-2000 polarimeter (Tokyo, Japan), operating with a tungsten lamp at a wavelength of 589 nm at 20 °C. Melting points were recorded on a digital Marconi MA-381 (Piracicaba, Brazil) apparatus and were uncorrected. Fourier-transform infrared (FTIR) spectra were obtained on a PerkinElmer Spectrum 100 spectrometer (Waltham, USA), using a universal attenuated total reflectance accessory (UATR). The high-resolution mass spectra (HRMS) analysis was acquired on a chromatograph coupled to an ion trap mass spectrometer and time-of-flight (LCMS-IT-TOF, Shimadzu, Kyoto, Japan) system as well as an Acquity UPLC instrument coupled to a Xevo QToF mass analyzer (Waters, Milford, MA, USA). ¹H and ¹³C NMR (1D and 2D) spectra were run on a Bruker Avance DRX-500 spectrometer, using MeOD and C₅D₅N

(Cambridge Isotope Laboratories Inc., Tewksbury, USA) as solvents. The high-performance liquid chromatography (HPLC) separations were achieved on a Shimadzu-UFLC semi-preparative HPLC system, equipped with ternary pumps and diode array SPD-M20A UV/VIS detector using a Phenomenex C18 column (Phenomenex, Torrance, USA) (250 × 10 mm, 5 mm) and a mobile phase consisting of water was purified in a Milli-Q system (Millipore, St. Louis, USA) with trifluoroacetic acid (CF₃CO₂H, 0.1% v/v) analytical grade was acquired from Vetec (Rio de Janeiro, Brazil) and acetonitrile (MeCN) HPLC grade, were purchased from Tedia (Rio de Janeiro, Brazil), a flow rate of 4.7 or 4.0 mL min⁻¹, oven temperature of 40 °C, monitored at 210-400 nm. Chromatography columns (CC) were performed using silica gel 60 (70-230 mesh, Vetec, Rio de Janeiro, Brazil), while the analytical thin-layer chromatography (TLC) was carried out on pre-coated TLC silica gel plates (Merck, Frankfurt, Germany) and the spots visualized by spraying with a vanillin/perchloric acid/EtOH (Vetec, Rio de Janeiro, Brazil and Merck, Frankfurt, Germany) solution followed by heating at 100 °C. All PA solvents were purchased from Labsynth (São Paulo, Brazil).

Plant material

Cordia glazioviana was collected in April 2012 at Acarape county, Ceará State, Brazil and was authenticated by Dra Maria Iracema Bezerra Loiola, botanist of Departamento de Biologia, Universidade Federal do Ceará (UFC). A voucher specimen (No. 30824) is deposited at the Herbário Prisco Bezerra-UFC. The collection permit was granted by Biodiversity Authorization and Information, SisGen number A86B918.

Extraction and isolation

The air-dried and milled heartwood (2.7 kg) of *C. glazioviana* was macerated with EtOH (3 × 10 L), at room temperature for 24 h and the resulting solutions were distilled under reduced pressure to yield 91.8 g of the crude extract. The EtOH extract was solubilized in a mixture of MeOH-H₂O 2:1 and partitioned with *n*-hexane, dichloromethane (CH₂Cl₂) and ethyl acetate (EtOAc) to yield the respective fractions: CGH (21.8 g), CGD (26.7 g) and CGA (7.5 g). The CGD fraction was fractionated on a silica gel column (55.1 g) eluting with *n*-hexane-EtOAc (8:2, 6:4, 4:6, 2:8, v/v), EtOAc-MeOH (8:2, 6:4, v/v) and MeOH, to yield fractions CGDF1-F7. CGDF1 (900.0 mg) was subjected to a silica gel CC eluted with *n*-hexane, *n*-hexane-EtOAc (9.5:0.5, 9:1, 8:2, 7:3, 6:4, 1:1, v/v) and EtOAc to afford 51 fractions (20 mL each), which were

pooled into 5 main subfractions (CGDF1a-CGDF1e) after TLC analysis. CGDF1a (91.2 mg) was subjected to a flash chromatography column eluted with *n*-hexane-EtOAc 1:1 (v/v) to yield compound **10** (6.0 mg). CGDF1b (78.0 mg) was purified by HPLC using a semi-preparative column and an isocratic solvent system of H₂O-MeCN 1:1 at a flow rate of 4.5 min⁻¹ to afford **8** (8.0 mg, retention time (t_R) 10.2 min) and **9** (10.1 mg, t_R 15.9 min). CGDF1d (106.1 mg) was applied to a silica gel column and eluted with *n*-hexane-CH₂Cl₂ (8:2, 6:4, 4:6, 2:8, v/v), CH₂Cl₂, CH₂Cl₂-EtOAc (9:1, 7:3, 1:1, 3:7, 1:9, v/v) and EtOAc to give 83 fractions of 8 mL each, pooled into 6 main fractions after TLC analysis. Fraction *n*-hexane-CH₂Cl₂ (4:6, v/v), afforded compound **11** (16.2 mg). CGDF2 (2.1 g) was subjected to a silica gel column eluted with *n*-hexane, *n*-hexane-EtOAc (9.5:0.5, 9:1, 8:2, 7:3, 6:4, v/v) and EtOAc, to yield fractions CGDF2a-CGDF2f after TLC monitoring. Fraction CGDF2c (1.0 g) was fractionated over silica gel by elution with *n*-hexane-CH₂Cl₂ (9:1, 8:2, 7:3, 6:4, 1:1, 4:6, 3:7, 2:8, v/v) and CH₂Cl₂ to yield 70 fractions, which were pooled into 7 subfractions. HPLC analysis of subfraction *n*-hexane-CH₂Cl₂ 7:3 (171.0 mg) on a C₁₈ semi-preparative column using a solvent system gradient (H₂O-MeCN 1:1→3:7 in 20 min) at a flow rate of 4.5 min⁻¹, to yield compound **7** (2.4 mg, t_R 13.2 min). CGDF2d (1.1 g) was chromatographed over silica gel and eluted with *n*-hexane-CH₂Cl₂ (8:2, 6:4, 4:6, 2:8, v/v), CH₂Cl₂, CH₂Cl₂-EtOAc (8:2, 6:4, v/v) to give 68 fractions (30 mL each), which were pooled into 5 main fractions (CGDF2d1-CGDF2d5) after TLC analysis. CGDF2d2 was chromatographed over silica gel, eluting with *n*-hexane-CH₂Cl₂ (8:2, 6:4, 4:6, 2:8, v/v), CH₂Cl₂, CH₂Cl₂-EtOAc (8:2, 6:4, 4:6, v/v) to yield 77 fractions (5 mL each), which were combined according to their TLC profile in 4 subfractions. Subfraction 1 (150.2 mg) was analyzed by HPLC using a C₁₈ semi-preparative column and an aqueous solution of 0.1% CF₃CO₂H in MeCN (65:35→40:60 in 25 min) as eluent, with a flow rate of 4.0 mL min⁻¹, to yield **6** (5.3 mg, t_R 15.9 min) and **2** (6.1 mg, t_R 17.3 min). The subfraction 4 (81.7 mg) was fractionated over silica eluted with *n*-hexane-CH₂Cl₂ (1:1, 4:6, 3:7, 2:8, 1:9, v/v), CH₂Cl₂, CH₂Cl₂-EtOAc (9:1, 8:2, 7:3 v/v) to afford compound **1** (10.0 mg) from subfraction *n*-hexane-CH₂Cl₂ (2:8). CGDF2e (350.0 mg) was chromatographed on a silica gel column eluting with *n*-hexane-CH₂Cl₂ (7:3, 1:1, 3:7, 1:9, v/v) and CH₂Cl₂/EtOAc (9:1, 7:3, 1:1, v/v) to yield subfractions CGDF2e1-CGDF2e7. Compound **3** (12.0 mg) was isolated from CGDF2e7, while **4** (6.0 mg, t_R 11.5 min) was obtained from subfraction CGDF2e6 (176.5 mg) after C₁₈ semipreparative HPLC (H₂O-MeCN 6:4). The CGA fraction (7.5 g) was fractionated on a silica

gel column eluted with *n*-hexane-EtOAc (8:2, 7:3, 6:4, 1:1, 4:6, 3:7 and 2:8, v/v) to yield CGAF1-CGAF7. CGAF2 was subjected to a silica gel CC eluted with *n*-hexane-EtOAc (9:1, 8.5:1.5, 8:2, 7.5:2.5, 7:3, 6:4, 1:1, 4:6 and 3:7) to afford 147 subfractions (8 mL each). Subfractions 125-142 (114.6 mg) was subjected to a flash chromatography using *n*-hexane-EtOAc 4:6 and further purified by HPLC using a C₁₈ semi-preparative column with the solvent system H₂O-MeCN (75:25→55:45 in 20 min) and a flow rate of 4.0 mL min⁻¹ to afford compound **5** (9.8 mg, t_R 17.2 min).

Computational details

To establish the relative stereochemistry of compounds **3** and **5**, two possible isomers of each one of those compounds (**3a/3b** and **5a/5b**) were drawn and their geometrical structures were optimized by using standard techniques.²⁷ Optimization calculations were performed by using density functional theory (DFT)²⁸ method and a functional version of the PW91 exchange in combination with the original PW91 correlation functional and a mixing ratio of exact and DFT exchange of 0.25:0.75, mPW1PW91²⁹ along with 6-31G(d,p) basis set implemented in Gaussian 16 package.³⁰ The frequencies of the optimized geometries were calculated to determine whether the resulting geometries were true minima or transition states on the potential energy surface. All optimization calculations were performed in solution by using the polarizable continuum model (PCM)³¹ with the integral equation formalism (IEF)³² using methanol as solvent. The NMR isotropic shielding constants were determined from the optimized geometries of **3a/3b** and **5a/5b** with mPW1PW91/6-31G(d,p) level of theory based on the GIAO¹⁴ proposal with tetramethylsilane (TMS) as reference implemented in the Gaussian 16.³⁰ The integral equation formalism and polarizable continuum model (IEF-PCM) solvation method was used with methanol (the solvent used to acquire the ¹H and ¹³C NMR spectra) as an implicit solvent to simulate the medium on the chemical shifts of the stereoisomers. A supplemental analysis that correlates NMR chemical shifts and statistical analysis, named DP4+ allows the use of quantum chemical calculated NMR parameters combined with refined statistical data to elucidate the most likely structure among the stereoisomers.¹⁵

Assay for cell viability

Cell viability was assessed using the MTT (Sigma-Aldrich, St. Louis, USA) assay as described previously.²⁵ In brief, RAW 264.7 cells (Merck, Frankfurt, Germany) were seeded into a 96-well plate at a density of 1 × 10⁴ cells *per* well and incubated at 37 °C for 24 h. Compounds at

different concentrations (12.5-100 μM) in dimethyl sulfoxide (DMSO, Romil Chemical Ltd., Cambridge, UK) were added to the cell plate for another 24 h, and then MTT (0.5 mg mL⁻¹) in phosphate-buffered saline (PBS, Merck, Frankfurt, Germany) was added into each well to form the formazan crystals (3 h). The supernatant was then carefully removed, and 100 μL of DMSO was added into each well to dissolve the MTT formazan crystals and measured at 540 nm using a microplate reader.

Assay for the inhibition of cellular NO production

The nitrite concentration in the medium was measured by the Griess reagent as an indicator of NO production.²⁶ RAW 264.7 cells were seeded into a 96-well plate at a density of 5 × 10⁵ cells *per* well and incubated at 37 °C for 24 h. After that, the cells were treated with several sample concentrations (6.25-50 μM) or controls (0.01% DMSO or 4 μM dexamethasone) for 2 h and then incubated with 1 μg mL⁻¹ LPS for 24 h. To measure the NO in the culture medium, a total of 100 μL of culture medium from each sample was mixed with the same volume of Griess reagent and incubated at 37 °C for 10 min. The absorbance was measured at 540 nm using a microplate reader.

Cordiaquinol D (**1**)

Yellow resin; [α]_D²⁰ -22.0 (*c* 0.1, MeOH); IR (ATR) ν_{max} / cm⁻¹ 3405, 1698, 1630, 1490, 1442, 1362, 1292, 1222, 929, 881; ¹H and ¹³C NMR data, see Table 1; HRESIMS *m/z*, calcd. for C₁₇H₁₇O₅ [M - H]⁻: 301.1081, found: 301.1076.

Cordiaquinol E (**2**)

Yellow resin; [α]_D²⁰ +16.0 (*c* 0.1, acetone); IR (ATR) ν_{max} / cm⁻¹ 3412, 1674, 1631, 1467, 1257, 1214; ¹H and ¹³C NMR data, see Table 1; HRESIMS *m/z*, calcd. for C₁₆H₁₇O₄ [M - H]⁻: 273.1132, found: 273.1129.

(10*R*)-10,11-Dihydrofuran-1,4-dihydroxy-globiferin (**3**)

Yellow resin; [α]_D²⁰ +2.7 (*c* 0.06, acetone); IR (ATR) ν_{max} / cm⁻¹ 3362, 1649, 1466, 1264, 780, 703; ¹H and ¹³C NMR data, see Table 1; HRESIMS *m/z*, calcd. for C₁₆H₁₉O₃ [M + H]⁺: 259.1429, found: 259.1418.

2-[(1'*E*,6'*E*)-3',8'-Dihydroxy-3',7'-dimethylocta-1',6'-dienyl]-benzene-1,4-diol (**4**)

Colorless resin; [α]_D²⁰ +9.2 (*c* 0.1, acetone); IR (ATR) ν_{max} / cm⁻¹ 3307, 2967, 2918, 1484, 1456, 1203, 955, 918, 763, 711; ¹H and ¹³C NMR spectral data, see Table 3; HRESIMS *m/z*, calcd. for C₁₆H₁₉O₂ [M + H - 2H₂O]⁺: 243.1380, found: 243.1381.

6-[(2'*R*)-2'-Hydroxy-3',6'-dihydro-2*H*-pyran-5'-yl]-2-methoxy-7-methylnaphthalene-1,4-dione (**5**)

Yellow resin; $[\alpha]_D^{20}$ -16.0 (c 0.1, MeOH); IR (ATR) ν_{\max} / cm^{-1} 3411, 2927, 1683, 1649, 1606, 1295, 1250, 906, 852; ^1H and ^{13}C NMR data, see Table 3; HRESIMS m/z , calcd. for $\text{C}_{17}\text{H}_{15}\text{O}_5$ $[\text{M} - \text{H}]^-$: 299.0925, found: 299.0920.

Supplementary Information

Supplementary data are available free of charge at <http://jbcs.s bq.org.br> as a PDF file.

Acknowledgments

This study was financed by Coordenação de Aperfeiçoamento de Pessoal de Nível Superior Brasil (CAPES), finance code 001/Fundação Cearense de Apoio ao Desenvolvimento Científico e Tecnológico (FUNCAP, No. 88887.113263/2015-01), Instituto Nacional de Ciência e Tecnologia (INCT BioNat, No. 465637/2014-0), and Conselho Nacional de Desenvolvimento Científico e Tecnológico (CNPq, 309060/2016-8). The authors thank High-Performance Computing Center (NPAD) at Federal University of Rio Grande do Norte (UFRN) and the National High-Performance Processing Center of the Federal University of Ceará (UFC) for providing computational resources and to CNPq for financial support and the researcher fellowships.

Author Contributions

AKOS performed the chemical experiments supervised by ODLP; RACS and FAS performed the biological experiments; FCLP, RBF, ERS and KMC performed the NMR and HRMS analyses; NKVM performed the theoretical analysis. ODLP, FAS, KMC, NKVM, and ERS contributed to the writing of the manuscript and its revision.

References

- Giles-Rivas, D.; Estrada-Soto, S.; Aguilar-Guadarrama, A. B.; Almanza-Pérez, J.; García-Jiménez, S.; Colín-Lozano, B.; Navarrete-Vázquez, G.; Villalobos-Molina, R.; *J. Ethnopharmacol.* **2020**, *251*, 112543.; Matias, E. F. F.; Alves, E. F.; Silva, M. K. N.; Carvalho, V. R. A.; Coutinho, H. D. M.; Costa, J. G. M.; *Braz. J. Pharmacog.* **2015**, *25*, 542.
- Oza, M. J.; Kulkarni, Y. A.; *J. Pharm. Pharmacol.* **2017**, *69*, 755.
- Dutra, R. C.; Campos, M. M.; Santos, A. R. S.; Calixto, J. B.; *Pharmacol. Res.* **2016**, *112*, 4.
- Basting, R. T.; Spindola, H. M.; Sousa, I. M. O.; Queiroz, N. C. A.; Trigo, J. R.; Carvalho, J. E.; Foglio, M. A.; *Biomed. Pharmacother.* **2019**, *112*, 108693; Castro, J.; Rivera, D.; Franco, L. A.; *J. Pharm. Invest.* **2018**, *49*, 331; Gupta, R.; Gupta, G.; *Pharmacogn. J.* **2017**, *9*, 93.
- Matos, T. S.; Silva, A. K. O.; Quintela, A. L.; Pinto, F. C. L.; Canuto, K. M.; Filho, R. B.; Fonseca, M. J. S.; Luna-Costa, A. M.; Paz, I. A.; Nascimento, N. R. F.; Silveira, E. R.; Pessoa, O. D. L.; *Fitoterapia* **2017**, *123*, 65.
- Costa, J. G. M.; Pessoa, O. D. L.; Monte, F. J. Q.; Menezes, E. A.; Lemos, T. L. G.; *Quim. Nova* **2005**, *28*, 591.
- Hu, S.; Ma, Y. L.; Guo, J. M.; Wen, Q.; Yan, G.; Yang, S.; Fu, Y. H.; Liu, Y. P.; *Nat. Prod. Res.* **2020**, *34*, 3499; Medeiros, R.; Passos, G. F.; Vitor, C. E.; Koepf, J.; Mazzuco, T. L.; Pianowski, L. F.; Campos, M. M.; Calixto, J. B.; *Br. J. Pharmacol.* **2007**, *151*, 618; Fernandes, E. S.; Passos, G. F.; Medeiros, R.; Cunha, F. M.; Ferreira, J.; Campos, M. M.; Pianowski, L. F.; Calixto, J. B.; *Eur. J. Pharmacol.* **2007**, *569*, 228.
- Wang, J.; Jin, M.; Jin, C.; Ye, C.; Zhou, Y.; Wang, R.; Cui, H.; Zhou, W.; Li, G.; *Nat. Prod. Res.* **2020**, *34*, 3313; Vinh, L. B.; Jang, H. J.; Phong, N. V.; Cho, K.; Park, S. S.; Kang, J. S.; Kim, Y. H.; Yang, S. Y.; *Bioorg. Med. Chem. Lett.* **2019**, *29*, 965.
- Yang, C.; Liu, P.; Wang, S.; Zhao, G.; Zhang, T.; Guo, S.; Jiang, K. F.; Wu, H. C.; Deng, G.; *Biochem. Biophys. Res. Commun.* **2018**, *505*, 1; Yi, Y. S.; Kim, M. Y.; Cho, J. Y.; *Korean J. Physiol. Pharmacol.* **2017**, *21*, 345.
- Soares, A. S.; Barbosa, F. L.; Rüdiger, A. L.; Hughes, D. L.; Salvador, M. J.; Zampronio, A. R.; Stefanello, M. E. A.; *J. Nat. Prod.* **2017**, *80*, 1837.
- Gottschling, M.; Miller, J. S.; *Syst. Bot.* **2006**, *31*, 361.
- Costa, J. G. M.; Magalhães, H. I. F.; Lemos, T. L. G.; Pessoa, O. D. L.; Pinheiro, G. M.; *Rev. Bras. Farmacogn.* **2002**, *12*, 68.
- Dettrakul, S.; Surerum, S.; Rajviroongit, S.; Kittakoop, P.; *J. Nat. Prod.* **2009**, *72*, 861.
- Wolinski, K.; Hinton, J. F.; Pulay, P.; *J. Am. Chem. Soc.* **1990**, *112*, 8251.
- Grimblat, N.; Zanardi, M. M.; Sarotti, A. M.; *J. Org. Chem.* **2015**, *80*, 12526; Smith, S. G.; Goodman, J. M.; *J. Am. Chem. Soc.* **2010**, *132*, 12946.
- Ioset, J. R.; Marston, A.; Gupta, M. P.; Hostettmann, K.; *J. Nat. Prod.* **2000**, *63*, 424.
- Pessoa, O. D. L.; Lemos, T. L. G.; Carvalho, M. G.; Braz-Filho, R.; *Phytochemistry* **1995**, *40*, 1777.
- Pretsch, E.; Bühlmann, P.; Affolter, C.; *Structure Determination of Organic Compounds Tables of Spectra Data*, 2nd ed.; Springer: Berlin, 2000.
- Simon-Levert, A.; Arrault, A.; Bontemps-Subielos, N.; Canal, C.; Banigs, B.; *J. Nat. Prod.* **2005**, *68*, 1412.
- Mahmoud, A. A.; *Phytochemistry* **1997**, *45*, 1633.
- Kamel, A.; *J. Nat. Prod.* **1995**, *58*, 428.

22. Figueroa, M.; Raja, H.; Falkinham, J. O.; Adcock, A. F.; Kroll, D. J.; Wani, M. C.; Pearce, C. J.; Oberlies, N. H.; *J. Nat. Prod.* **2013**, *76*, 1007.
23. Hashidoko, Y.; Tahara, S.; Mizutani, J.; *Phytochemistry* **1992**, *31*, 2148.
24. Widhalm, J. R.; Rhodes, D.; *Hortic. Res.* **2016**, *3*, 16046; Dewick, P. M.; *Medicinal Natural Products, A Biosynthetic Approach*, 3rd ed.; Wiley: New York, 2009.
25. Mosmann, T.; *J. Immunol. Methods* **1983**, *65*, 55.
26. Green, L. C.; Wagner, D. A.; Glogowski, J.; Skipper, P. L.; Wishnok, J. S.; Tannenbaum, S. R.; *Anal. Biochem.* **1982**, *126*, 131.
27. Chambers, L. G.; Fletcher, R.; *Math. Gaz.* **2001**, *85*, 562.
28. Zinola, C. F.; *Electrocatalysis: Computational, Experimental, and Industrial Aspects*, 1st ed.; Zinola, C. F., ed.; CRC Press: Boca Raton, 2010.
29. Perdew, J. P.; Burke, K.; Ernzerhof, M.; *Phys. Rev. Lett.* **1996**, *77*, 3865.
30. Frisch, M. J.; Trucks, G. W.; Schlegel, H. B.; Scuseria, G. E.; Robb, M. A.; Cheeseman, J. R.; Scalmani, G.; Barone, V.; Petersson, G. A.; Nakatsuji, H.; Li, X.; Caricato, M.; Marenich, A. V.; Bloino, J.; Janesko, B. G.; Gomperts, R.; Mennucci, B.; Hratchian, H. P.; Ortiz, J. V.; Izmaylov, A. F.; Sonnenberg, J. L.; Williams-Young, D.; Ding, F.; Lipparini, F.; Egidi, F.; Goings, J.; Peng, B.; Petrone, A.; Henderson, T.; Ranasinghe, D.; Zakrzewski, V. G.; Gao, J.; Rega, N.; Zheng, G.; Liang, W.; Hada, M.; Ehara, M.; Toyota, K.; Fukuda, R.; Hasegawa, J.; Ishida, M.; Nakajima, T.; Honda, Y.; Kitao, O.; Nakai, H.; Vreven, T.; Throssell, K.; Montgomery Jr., J. A.; Peralta, J. E.; Ogliaro, F.; Bearpark, M. J.; Heyd, J. J.; Brothers, E. N.; Kudin, K. N.; Staroverov, V. N.; Keith, T. A.; Kobayashi, R.; Normand, J.; Raghavachari, K.; Rendell, A. P.; Burant, J. C.; Iyengar, S. S.; Tomasi, J.; Cossi, M.; Millam, J. M.; Klene, M.; Adamo, C.; Cammi, R.; Ochterski, J. W.; Martin, R. L.; Morokuma, K.; Farkas, O.; Foresman, J. B.; Fox, D. J.; *Gaussian 16*, Revision C.01, Inc., Wallingford CT, 2016.
31. Mennucci, B.; *Wiley Interdiscip. Rev.: Comput. Mol. Sci.* **2012**, *2*, 386.
32. Mennucci, B.; Cancès, E.; Tomasi, J.; *J. Phys. Chem. B* **1997**, *101*, 10506.

Submitted: August 19, 2020

Published online: March 31, 2021

